CrossMark

Comet 240P/NEAT Is Stirring

Michael S. P. Kelley[1] ![ORCID], Dennis Bodewits[2] ![ORCID], Quanzhi Ye (叶泉志)[3,4] ![ORCID], Tony L. Farnham[1] ![ORCID], Eric C. Bellm[5] ![ORCID],
Richard Dekany[6], Dmitry A. Duev[3] ![ORCID], George Helou[4], Thomas Kupfer[7] ![ORCID], Russ R. Laher[4] ![ORCID], Frank J. Masci[4] ![ORCID],
Thomas A. Prince[3] ![ORCID], Ben Rusholme[4] ![ORCID], David L. Shupe[4] ![ORCID], Maayane T. Soumagnac[8] ![ORCID], and Jeffry Zolkower[6]

[1] Department of Astronomy, University of Maryland, College Park, MD 20742-0001, USA; msk@astro.umd.edu
[2] Physics Department, Leach Science Center, Auburn University, Auburn, AL 36832, USA
[3] Division of Physics, Mathematics, and Astronomy, California Institute of Technology, Pasadena, CA 91125, USA
[4] Infrared Processing and Analysis Center, California Institute of Technology, Pasadena, CA 91125, USA
[5] DIRAC Institute, Department of Astronomy, University of Washington, 3910 15th Avenue NE, Seattle, WA 98195, USA
[6] Caltech Optical Observatories, California Institute of Technology, Pasadena, CA 91125, USA
[7] Kavli Institute for Theoretical Physics, University of California, Santa Barbara, CA 93106, USA
[8] Benoziyo Center for Astrophysics, Weizmann Institute of Science, Rehovot, Israel

Abstract

Comets are primitive objects that formed in the protoplanetary disk, and have been largely preserved over the history of the solar system. However, they are not pristine, and surfaces of cometary nuclei do evolve. In order to understand the extent of their primitive nature, we must define the mechanisms that affect their surfaces and comae. We examine the lightcurve of comet 240P/NEAT over three consecutive orbits, and investigate three events of significant brightening ($\Delta m \sim -2$ mag). Unlike typical cometary outbursts, each of the three events are long-lived, with enhanced activity for at least 3–6 months. The third event, observed by the Zwicky Transient Facility, occurred in at least two stages. The anomalous behavior appears to have started after the comet was perturbed by Jupiter in 2007, reducing its perihelion distance from 2.53 to 2.12 au. We suggest that the brightening events are temporary transitions to a higher baseline activity level, brought on by the increased insolation, which has warmed previously insulated sub-surface layers. The new activity is isolated to one or two locations on the nucleus, indicating that the surface or immediate sub-surface is heterogeneous. Further study of this phenomenon may provide insight into cometary outbursts, the structure of the near-surface nucleus, and cometary nucleus mantling.

Unified Astronomy Thesaurus concepts: Cometary studies (279); Light curves (918)

1. Introduction

Cometary nucleus surfaces are dynamic, with many processes affecting their volatile content, strength, particle size distribution, and mass loss (Thomas et al. 2013, 2015; Veverka et al. 2013; El-Maarry et al. 2015; Sunshine et al. 2016). Most processes are ultimately driven by insolation. This fact enables the study of nuclear surfaces through examination of gas and dust production as they rotate and orbit the Sun. The correlation of composition or mass-loss rates with insolation may reveal the composition, structure, or evolution of the near-surface layer (e.g., Biver et al. 1997; Meech et al. 2013; Bodewits et al. 2014; Feaga et al. 2014).

Gradual and repeated variations occur on seasonal and diurnal timescales as localized sources on the nucleus vary in activity (e.g., Hayward et al. 2000; Schleicher 2007; A'Hearn et al. 2011; Kramer et al. 2017). In contrast, cometary outbursts are more stochastic. These impulsive increases in mass-loss rate eject material into the coma, causing an immediate and rapid brightening in telescopic observations. The total brightness of the coma varies with a near-exponential decay as the outburst ejecta slowly leaves the vicinity of the nucleus (Hughes 1990). The causes of outbursts vary (Hughes 1991). For example, they may be driven by sub-surface energy storage (Agarwal et al. 2017), rotationally induced mass shedding (Steckloff & Samarasinha 2018), cliff collapse (Pajola et al. 2017), and water ice phase state transitions (Prialnik & Bar-Nun 1990; Belton & Melosh 2009). On occasion, outbursts signal the complete disruption of the nucleus (Farnham et al. 2001; Knight & Battams 2014; Li & Jewitt 2015).

Comet 240P/NEAT is a Jupiter-family comet, discovered in 2002 as P/2002 X2 by the Near-Earth Asteroid Tracking (NEAT) survey with the 1.2 m Samuel Oschin telescope at Palomar Observatory (Lawrence et al. 2002). With a 7.6 yr orbital period, it has been observed over three perihelion passages. On 2007 July 10, it made a close approach to Jupiter ($\Delta_J = 0.25$ au, heliocentric distance $r_h = 5.5$ au) and its perihelion distance, q, dropped from 2.53 to 2.12 au (NASA JPL Small-Body Database, orbital solution JPL K182/8), corresponding to a 40% increase in insolation at perihelion. Prior to this encounter, the comet's orbit had been stable with q near 2.5–2.6 au for at least 80 yr, according to the same JPL solution.

After passing through perihelion in the newly perturbed orbit, an apparent 2 mag outburst was reported by B. Haeusler,[9] occurring between 2011 March 29 and April 6. On the next perihelion passage, a second apparent 2 mag outburst was reported by Sato (2017), between 2017 July 18.63 and August 28.59 UTC. In 2018, S. Yoshida (2019, personal communication) received a report from T. Ikemura and H. Sato (at Shinshiro, IAU observatory code Q11) that the comet had experienced a third apparent outburst, 1–2 mag in strength, between 2018 November 14.81 and December 12.68 UTC.

We examine the apparent outbursts and baseline activity of comet 240P. We present photometry of the comet from the Zwicky Transient Facility (ZTF; Bellm et al. 2019; Graham et al. 2019), the Palomar Transient Factory (PTF;

---

[9] https://groups.yahoo.com/neo/groups/comets-ml/conversations/messages/17241

Law et al. 2009; Rau et al. 2009), and the NEAT survey. These data, in combination with photometry reported to the Minor Planet Center (MPC), reveal a comet in repeated transition between two different activity states.

2. Observations and Results

The ZTF is a time-domain all-sky survey and successor to the PTF. First light was acquired 2017 November 1, and science operations commenced 2018 March 20. The camera utilizes 16 6k×6k CCDs (1″01 per pixel) to cover a 47 square degree field of view. It is mounted on the 1.2 m Oschin Schmidt telescope at Palomar Observatory. Survey operations typically use 30 s exposures, allowing ZTF to cover 3800 square degrees an hour to a 5σ depth of $r = 20 - 21$ mag (Bellm et al. 2019; Graham et al. 2019).

We searched for observations of comet 240P/NEAT in the ZTF Data Release 1 and Partnership data archives (Masci et al. 2019) with the ZChecker program (Kelley et al. 2019). Survey coverage of the comet began on 2018 September 11.51 UTC at $r_h = 2.3$ au, 119 days after perihelion ($T_P = 2018$ May 15.88 UTC). It was also observed on two nights in December 2017 during ZTF's commissioning period. We inspected 63 ZTF g-, r-, and i-band images covering the comet, and measured its brightness using 15,000 km radius apertures. Several images were dropped from the analysis for various reasons, including stellar contamination, background artifacts, suspected clouds, or high background. The uniform aperture size was chosen to account for seeing and geocentric distance variations throughout the observation period (minimum aperture is 6″9, median seeing is 2″2). Photometry was calibrated to the PanSTARRS (PS1) data release 1 (DR1) catalog (Tonry et al. 2012) using the ZTF pipeline (Masci et al. 2019). We measured $g - r = 0.56 \pm 0.02$ mag from the average of seven g- and r-band image pairs; $r - i$ cannot be directly measured because the i-band images are separated from the other images by many days. We assume a constant spectral gradient from g to i, i.e., $r - i = 0.27$ mag. We used these values to color correct the data from the ZTF filters to the PS1 system (AB magnitudes). The results are binned by day (Table 1).

We also searched for comet 240P in the PTF archive with an online application at the Infrared Science Archive, and found eight images observed with an R-band filter. PTF image processing and photometric calibration is described by Laher et al. (2014) and Ofek et al. (2012). We calibrated the images to PS1 r-band magnitudes using background stars and the calviacat program (Kelley & Lister 2019). Photometry of the comet in 9″5 radius apertures is presented in Table 1. The fixed angular size was chosen to make the results more comparable to the MPC photometry (justified in Section 4.1).

In addition, we obtained all comet 240P photometry reported to the MPC (Williams 2019). The data were taken with a wide range of calibration methods, aperture sizes, and bandpasses. As a result, there is a large scatter in reported magnitudes, even when data are separated into "nuclear" (small) and "total" (whole coma) magnitudes. We select all photometry from a subset of observatories (360, 644, 693, 699, 704, E12, H45, G96, T08, T05, V06, 958, B96, H47, J38, B82, and A71), chosen for broad time coverage and the best-quality data. The remaining MPC data produce an improved lightcurve, but still have scatter at the magnitude level. However, activity trends are apparent in the data, therefore we include them in our analysis.

We also searched the data archived at the Canadian Astronomy Data Centre (Gwyn et al. 2012) for pre-discovery (2002) detections of 240P. The comet was covered by NEAT survey images on 1998 May 3 and May 24 ($r_h = 5.4$ au), but the predicted brightness ($V \sim 21$ mag) was below the sensitivity limit of the images ($V \sim 19$ mag). A search by eye on the images within the uncertainty ellipse ($<3''$) did not turn up any evidence for the object. We conclude that the comet was not more than 2 magnitudes brighter than the 2003 activity level at that time.

Three images of comet 240P on 2003 January 16 were found in the partial NEAT data archive of Bauer & Lawrence (2013). We bias-subtracted and flat-fielded the data, and measured the coma within 7″ radius apertures. The photometric aperture is limited due to a nearby star. The unfiltered images were calibrated to PS1 r-band magnitudes using background stars. The weighted-mean photometry is presented in Table 1.

3. Models

To model the comet's photometric behavior, we use the $Af\rho$ coma quantity of A'Hearn et al. (1984). It is proportional to the apparent brightness of the comet, and is defined as the product of grain albedo, filling factor within the aperture, and aperture size projected to the distance of the comet:

$$A(\theta)f\rho = \frac{4\Delta^2 r_h^2 F_\lambda}{\rho S_\lambda}, \qquad (1)$$

where $A(\theta)f\rho$ specifies that the measurement is for a specific phase angle θ, Δ is the observer-comet distance, F_λ is the observed spectral flux density of the coma within a circular aperture with projected linear radius ρ, and S_λ is the spectral flux density of sunlight at 1 au. Despite the units of length, $Af\rho$ is a proxy for the comet's intrinsic dust coma activity, i.e., mass-loss rate (Fink & Rubin 2012). To model the comet's brightness, we assume $Af\rho$ varies as a power law based on the heliocentric distance (r_h):

$$A(\theta)f\rho = A(0°)f\rho\Phi(\theta)\left(\frac{r_h}{q}\right)^k, \qquad (2)$$

where Φ is a phase function for light scattered by cometary dust (Schleicher & Bair 2011), q is the perihelion distance, and k is the power-law slope. $A(0°)f\rho$ is the value that would be measured if the comet were observed at a phase angle of $0°$.

We also interpret the comet's activity state with the ice sublimation model of Cowan & A'Hearn (1979). This model balances absorption of sunlight by a low-albedo (5% bond albedo) spherical nucleus with the energy losses of thermal radiation and ice sublimation. Based on spacecraft observations, cometary surfaces have low thermal inertias (Davidsson et al. 2013; Groussin et al. 2013; Gulkis et al. 2015); i.e., their surface temperatures are in near-instantaneous equilibrium with sunlight. We assume the same property for the nucleus of 240P in our ice sublimation model.

4. Analysis

4.1. 2018 Orbit: $T_P = 2018$ May 15.88 UTC

The ZTF photometry yields an unusual lightcurve with two apparent brightening events at $T_P + 172$ and $+185$ days (Figure 1). The first brightening had a strength of $\Delta m \sim -0.7$ mag, and

Table 1
Photometry of Comet 240P/NEAT

Date (UTC) (1)	$T - T_P$ (days) (2)	r_h (au) (3)	Δ (au) (4)	θ (°) (5)	N_{exp} (6)	t_{exp} (s) (7)	Airmass (8)	Seeing (″) (9)	ρ (″) (10)	Filter (11)	m (mag) (12)	σ_m (mag) (13)
Near-Earth Asteroid Tracking Survey												
2003 Jan 16 02:40	−72.50	2.573	2.254	22.27	3	180	1.22	3.8	7.0	r	18.52	0.07
Palomar Transient Factory												
2010 Jul 25 11:42	−70.78	2.196	2.575	22.85	1	60	2.30	2.7	9.50	r	16.79	0.09
2010 Sep 24 09:44	−9.87	2.125	1.895	28.16	2	120	1.77	2.7	9.50	r	16.05	0.06
2010 Dec 5 11:11	62.19	2.180	1.271	13.21	1	60	1.06	2.1	9.50	r	15.73	0.06
2010 Dec 7 05:20	63.95	2.183	1.266	12.49	2	120	1.65	2.8	9.50	r	15.69	0.04
2010 Dec 8 05:17	64.95	2.184	1.263	12.09	2	120	1.64	2.5	9.50	r	15.68	0.03
Zwicky Transient Facility												
2017 Dec 12 02:46	−154.76	2.442	2.235	23.77	1	180	1.90	3.7	9.26	r	16.01	0.02
2017 Dec 17 02:49	−149.76	2.425	2.275	23.90	1	240	1.90	3.5	9.09	r	16.06	0.02
2018 Sep 11 12:22	118.64	2.324	2.935	17.62	1	30	1.98	2.5	7.05	r	17.07	0.04
2018 Sep 14 12:20	121.64	2.333	2.918	18.04	1	30	1.88	2.6	7.09	r	17.14	0.04
2018 Sep 16 12:09	123.63	2.339	2.907	18.30	1	30	2.31	2.3	7.12	g	17.63	0.05
2018 Sep 26 11:39	133.61	2.370	2.847	19.54	1	30	2.17	2.3	7.27	r	17.25	0.07
2018 Sep 29 11:49	136.61	2.380	2.828	19.89	1	30	1.90	2.8	7.32	g	17.82	0.09
2018 Nov 3 12:35	171.65	2.503	2.571	22.50	1	30	1.29	3.6	8.05	g	17.40	0.05
2018 Nov 3 11:37	171.61	2.503	2.572	22.50	1	30	1.59	3.7	8.05	r	16.83	0.05
2018 Nov 7 11:24	175.60	2.518	2.539	22.60	1	30	1.57	2.1	8.15	g	17.45	0.04
2018 Nov 7 12:34	175.65	2.519	2.539	22.60	1	30	1.24	1.7	8.15	r	16.90	0.04
2018 Nov 8 13:07	176.67	2.522	2.531	22.62	1	30	1.09	2.0	8.18	g	17.47	0.04
2018 Nov 10 11:48	178.61	2.530	2.515	22.64	1	30	1.37	2.4	8.23	g	17.44	0.04
2018 Nov 10 12:54	178.66	2.530	2.515	22.64	1	30	1.15	2.3	8.23	r	16.90	0.03
2018 Nov 16 11:10	184.59	2.553	2.466	22.65	1	30	1.44	2.0	8.39	g	16.25	0.03
2018 Nov 17 11:40	185.61	2.557	2.458	22.64	1	30	1.31	1.9	8.42	g	16.19	0.03
2018 Nov 19 11:58	187.62	2.565	2.441	22.60	1	30	1.20	3.0	8.48	g	16.15	0.04
2018 Nov 19 12:34	187.65	2.565	2.441	22.60	1	30	1.11	2.2	8.48	r	15.59	0.03
2018 Nov 25 12:10	193.63	2.588	2.392	22.42	2	60	1.16	2.3	8.65	r	15.68	0.02
2018 Nov 27 10:53	195.57	2.596	2.376	22.34	1	30	1.34	1.6	8.71	r	15.76	0.04
2018 Nov 28 12:07	196.63	2.600	2.367	22.29	1	30	1.13	2.3	8.74	g	16.31	0.04
2018 Dec 9 11:55	207.62	2.644	2.280	21.48	1	30	1.07	2.0	9.07	g	16.44	0.03
2018 Dec 9 12:52	207.66	2.645	2.280	21.48	1	30	1.01	2.1	9.07	r	15.86	0.03
2018 Dec 15 11:51	213.62	2.669	2.235	20.85	1	30	1.09	1.7	9.26	g	16.40	0.07
2018 Dec 15 12:54	213.66	2.669	2.235	20.84	2	60	1.01	2.4	9.26	r	15.88	0.06
2018 Dec 16 12:24	214.64	2.673	2.228	20.72	1	30	1.03	2.0	9.29	r	15.87	0.02
2018 Dec 22 11:29	220.60	2.698	2.186	19.93	1	30	1.08	1.9	9.46	r	15.81	0.03
2018 Dec 24 10:45	222.57	2.706	2.173	19.64	1	30	1.13	1.9	9.52	r	15.76	0.03
2018 Dec 28 11:55	226.62	2.723	2.148	18.99	1	30	1.02	2.5	9.63	g	16.33	0.04
2018 Dec 29 11:06	227.58	2.727	2.142	18.83	1	30	1.06	3.0	9.66	r	15.75	0.03
2018 Dec 30 13:00	228.66	2.731	2.136	18.64	1	30	1.00	2.1	9.69	g	16.41	0.04
2019 Jan 9 10:52	238.57	2.773	2.085	16.79	1	30	1.03	1.6	9.93	r	15.89	0.04
2019 Jan 10 10:42	239.57	2.778	2.080	16.59	1	30	1.04	1.8	9.95	r	15.94	0.03
2019 Jan 24 12:11	253.63	2.838	2.039	13.73	1	30	1.03	3.1	10.15	g	16.52	0.05
2019 Feb 8 10:57	268.58	2.902	2.040	11.29	2	60	1.05	2.5	10.14	g	16.59	0.02
2019 Mar 15 08:26	303.47	3.055	2.249	12.76	1	30	1.07	3.0	9.20	i	16.29	0.04
2019 Mar 25 08:27	313.47	3.099	2.358	14.19	1	30	1.14	1.9	8.77	i	16.70	0.04
2019 Apr 9 07:27	328.43	3.164	2.554	16.05	1	30	1.13	1.4	8.10	i	17.16	0.05
2019 Apr 12 05:51	331.37	3.177	2.596	16.34	1	30	1.02	1.6	7.97	i	17.02	0.04
2019 Apr 23 08:14	342.46	3.226	2.763	17.19	1	30	1.48	1.9	7.49	i	17.45	0.06
2019 May 9 04:00	358.29	3.295	3.019	17.71	1	30	1.02	1.4	6.85	i	17.78	0.06
2019 May 25 04:07	374.29	3.364	3.288	17.46	4	120	1.08	1.9	6.29	i	17.96	0.04

Note. Column definitions: (1) mean observation date; (2) time from nearest perihelion date; (3) heliocentric distance; (4) observer–comet distance; (5) phase angle (Sun–target–observer); (6) number of exposures; (7) total exposure time; (8) mean airmass; (9) mean seeing (stellar FWHM); (10) photometric aperture radius; (11) filter bandpass, data from ZTF r and PTF R and NEAT (unfiltered) are calibrated to PS1 r, data from ZTF g are calibrated to PS1 g; (12) apparent magnitude; (13) uncertainty on m.
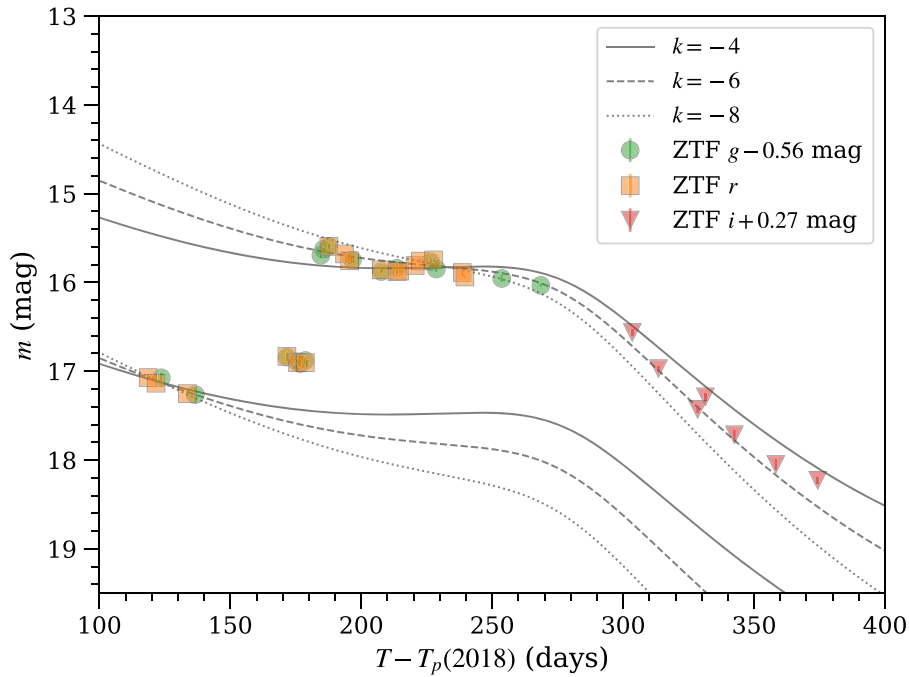
Figure 1. ZTF photometry of comet 240P/NEAT, measured with a 15,000 km radius aperture. Several photometric models are shown to demonstrate our model uncertainty on the heliocentric distance power-law slope, k.

occurred between T_P+136.6 and +171.6 days (September 29–November 3), where T_P is the perihelion date. After seven nights of a near-constant apparent magnitude, a second event occurred between T_P+178.7 and +184.6 days (November 10 and 16), increasing the total brightening to $\Delta m = -2$ mag. The latter event is the 2018 outburst identified by Ikemura and Sato (between T_P+182.9 and +210.8 days). These data indicate that the full 2 mag event was not simply a gradual increase in activity, but occurred in at least two stages. The apparent magnitude peaks on day three of the second event at +187.6 days. Subsequent structure in the lightcurve suggests a $\Delta m \sim -0.1$ mag peak near T_P+221 days.

Figure 1 presents lightcurves based on our $Af\rho$ model using the heliocentric distance slopes $k = -4$, -6, and -8. The lightcurves have the same aperture radius as the ZTF photometry (15,000 km). The data at $\sim T_P$+130 days cannot be used to discriminate between the three slopes (reduced χ^2 values are 0.4–0.6). However, $k = -6$ is the best of the three, and predicts $A(0°)f\rho = 213$ cm at perihelion.

None of our models account for the ~ 2 mag increase in activity at $\sim T_P$+180 days. Comparing this change in brightness to the $k = -4$ lightcurve implies the comet had a very slow return to quiescence, but even at T_P+350 days the comet is still -1.3 mag brighter than the model. The $k = -8$ lightcurve suggests the post-event brightening increased with time, up to 2.8 mag by T_P+350 days. Although there is no a priori requirement that any of these models fit the post-event lightcurve, the middle value, $k = -6$, is most consistent with it, and we adopt this slope for the remainder of the paper.

All three model lightcurves are nearly parallel to the ZTF photometry, which suggests that the event around $T_P + 180$ days was not a typical outburst, but rather a new sustained activity level. Good agreement with the data is obtained with the $k = -6$ model for $A(0°)f\rho(q) = 1346$ cm (Figure 1), equivalent to a factor of 6 increase in the dust production rate.

We examined the ZTF images to determine if the sustained brightening was due to lingering large grains, a new fragment, or to new activity. Images were averaged into three bins to enhance the data quality (pre-event: 2018 September 11–29 (five images); early-event: November 16–19 (five images); mid-event: 2019 February 2 (one image); late-event: March 15–April 9 (three images)). The results and azimuthally averaged profiles are presented in Figure 2. There is no morphological evidence for a new fragment. Before the event, the radial profile was close to $\rho^{-1.5}$, the canonical distribution of a tail-dominated image (Jewitt & Meech 1987). Immediately after the event, the profile was steeper than $\rho^{-1.5}$, which is indicative of an outburst early in its evolution when the ejecta is close to the nucleus. The radial profile returns to the pre-event distribution in the mid- and late-event images. An impulsive event cannot simultaneously have a $\rho^{-1.5}$ profile and a consistently high intrinsic brightness over this 130 day period, unless it were accompanied with new activity.

Figure 3 presents the long-term lightcurve of the comet based on the ZTF, PTF, and MPC photometry. Here, the ZTF photometry has been remeasured with a $9.''5$ radius aperture. This choice of aperture size produced photometry in agreement with the data reported by the Asteroid Terrestrial-impact Last Alert System (ATLAS) survey (Tonry et al. 2018), which accounts for most of the 2017/2018 photometry and informed our PTF photometric aperture choice. For this aperture size, the 2018 events increased the coma $Af\rho$ by a factor of ~ 9. The discrepancy with Figure 1, where a factor of ~ 6 change was found, is due to the limitations of the $Af\rho$ model, which assumes a $1/\rho$ surface brightness distribution.

Inspection of the pre-perihelion MPC data reveals the apparent outburst identified by Sato (2017) began between two sets of observations by ATLAS, at $T_P - 272.3$ and -270.3 days (2018 August 16 and 18). The ATLAS photometry suggest an outburst strength of 2–3 mag, followed by a 1–1.5 mag decay in 14 days. However, no ATLAS photometry
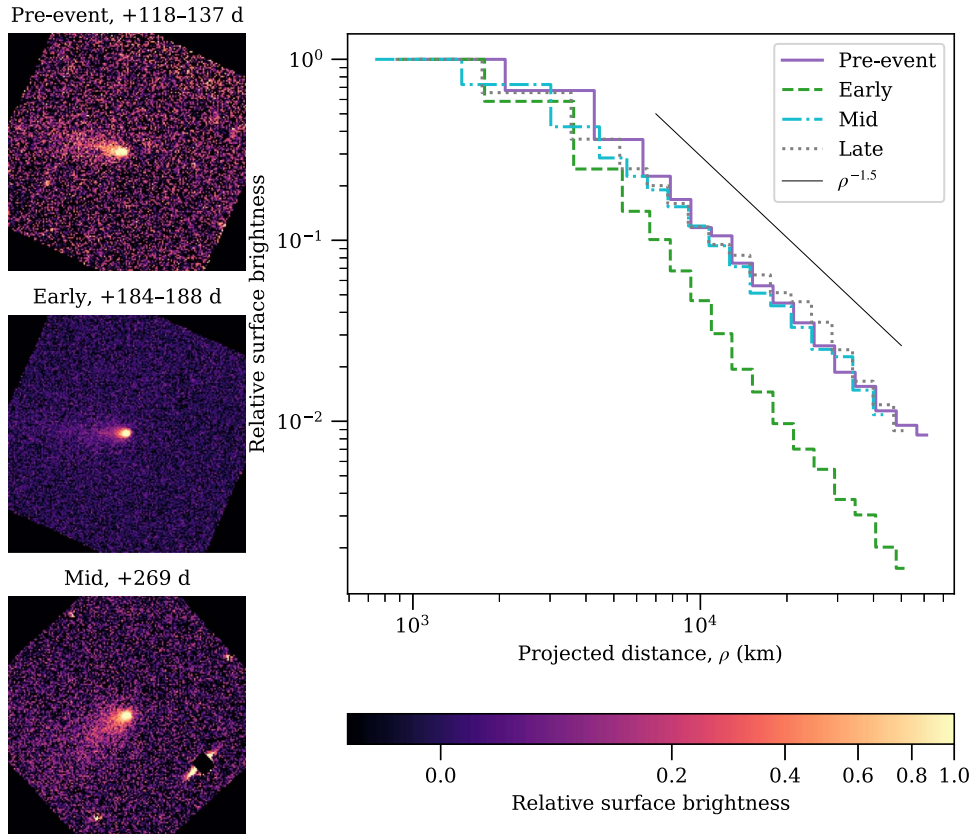
Figure 2. Left: ZTF images of comet 240P from the 2018 event (times are with respect to perihelion; see the text for details). The images are displayed normalized to the surface brightness in an 8″ radius aperture and the projected comet-Sun vector is to the right. Right: radial profiles for each image, plus an additional image from the late-event data ($T - T_p = 303-328$ days). Note that the first three bins are 1″, 2″, and 3″.

exists during this decay period. After the initially rapid fading, the coma takes around 80 days to reach the pre-outburst activity level, and continues to fade through the last data at 150 days after the outburst. This timescale is an order of magnitude longer than a typical cometary outburst (Hughes 1990). If the first ATLAS photometry points can be confirmed, it appears the event started with a typical outburst, but ended with an usually long fading period.

The pre- and post-perihelion events are separated by 220° of true anomaly. Based on solar illumination of the nucleus, it is possible that a single active area is responsible for both.

4.2. 2010 Orbit: $T_P = 2010$ October 04.27 UTC

An activity model with $A(0°)f\rho = 150$ cm at perihelion has good agreement with our PTF photometry, and parallels most of the MPC data in 2010–2011 (Figure 3). The outburst reported by Haeusler is clear in the MPC lightcurve at T_P+182 days. The data suggest the comet took 20 days to reach peak brightness, after which the coma remains near the 1350 cm model for 90 days, up to the last reported data for this period. This is the same part of the orbit as the 2018 brightening; both have on-set dates near +180 days. The portion of the orbit that covers the pre-perihelion event ($T_P - 270$ to -120 days) was not observed.

4.3. 2003 Orbit: $T_P = 2003$ March 29.61 UTC

The MPC photometric coverage in 2002–2004 covers $T_P - 180$ to -60 days, and $+247$ to $+353$ days. We examined these data for evidence of the 2011, 2017, and 2018 events.

Because the orbit changed after 2003, we plot the lightcurve versus ecliptic longitude of the comet-Sun vector, $\lambda_\odot$, under the assumption that the events are tied to specific illumination conditions on the nucleus. Figure 4 compares the ZTF photometry to the 2003 MPC and NEAT data using absolute magnitude:

$$H(1, 1, 0) = m - 5\log_{10}(r_h\Delta) - 2.5\log_{10}(\Phi(\theta)), \quad (3)$$

where Φ is the Halley-Marcus phase function from Schleicher & Bair (2011) evaluated at phase angle θ. Furthermore, the ZTF data are scaled to the 2003 circumstances using Equation (1). The pre-perihelion event would have spanned $\lambda_\odot = 165°-205°$, and its presence in 2003 cannot be tested. The post-perihelion events observed in 2011 and 2018 would have spanned from $\lambda_\odot = 305°$ to at least $350°$. Had this brightening occurred in the 2003 orbit, then we should have seen a comet near 18–19 mag, rather than the observed 20–21 mag. Either the event did not occur at that time, or it was much smaller in strength.

The 2003 lightcurve roughly agrees with $A(0°)f\rho \sim 40$ cm for $k = -6$ (Figure 4). A model following $A(0°)f\rho \sim 38$ cm for $k = -4$ (not shown) fits equally well. The lower activity level of this orbit is caused by the change in perihelion distance between 2003 and 2010. Scaling the 2010 estimate, $A(0°)f\rho \sim 150$ cm, by $(2.53/2.12)^{-6}$ yields 52 cm at perihelion.. This factor of 3 change is larger than the factor of 2 predicted by the water ice sublimation model of Cowan & A'Hearn (1979).
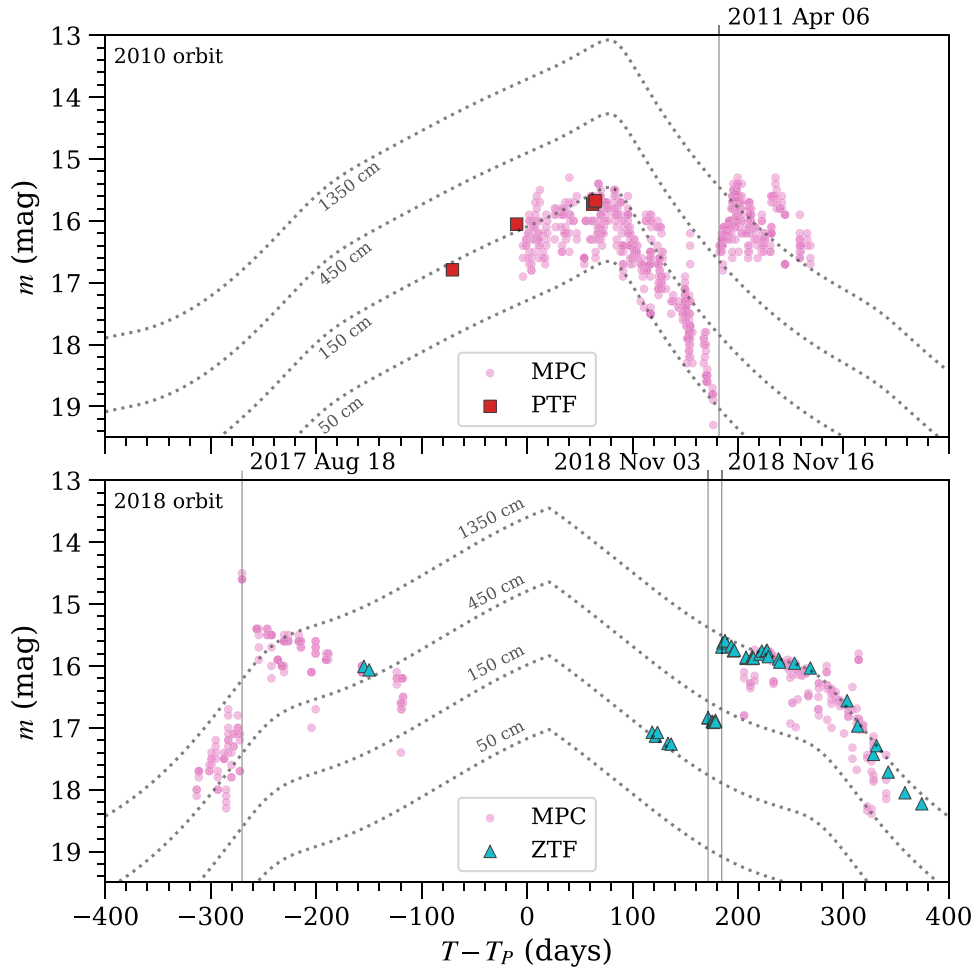
Figure 3. Lightcurve of comet 240P/NEAT vs. perihelion time ($T - T_P$) in 2010–2011 (top) and 2017–2018 (bottom). ZTF and PTF data are measured with $9\rlap{.}''5$ radius apertures. Select photometry contributed to the MPC are also shown (see Section 2 for details). Model lightcurves are presented (dotted lines), based on the $Af\rho$ formalism using the indicated value at perihelion ($9\rlap{.}''5$ aperture, $r_{\rm h}^{-6}$ scale factor). Approximate epochs of transition to increased activity levels are marked with vertical lines.

5. Discussion

The comet's behavior appears to have changed after the 2007 gravitational perturbation by Jupiter. In 2010, the comet returned to perihelion with a peak activity level nearly consistent with the reduced perihelion distance. 180 days after perihelion, the comet brightened by ~-2 mag, and remained bright for at least 90 days. In 2017, the comet again brightened by ~-2 mag, but this time slowly returned to a quiescent state, with a timescale much longer than is typical for outbursts, 150 versus 20–30 days (Hughes 1990). A third -2 mag brightening was observed in 2018, occurring in at least two stages over a 50 day period. The comet remained at this new activity level for 190 days, up to the end of our data set. Given these observations, we identify the following features of interest.

1. The comet brightened three times over two orbits, achieving nearly the same peak activity level each time: $A(0°)f\rho \sim 1350$ cm, corrected for heliocentric distance. This behavior is unusual for cometary outbursts at short-period comets, which have a power-law distribution in total mass (Ishiguro et al. 2016). To have three large events of the same order of magnitude is an indication that the same active area may be responsible for all events. A better understanding of this repeatability may

provide insight into possible outburst trigger mechanisms, or the near-surface structure of the active area in question.

2. The three brightening events all occurred after the 2007 orbital perturbation by Jupiter, which increased surface insolation at perihelion by 40% and the dust production rate by at least a factor of 3. The data from the 2003 orbit are sparse, but there is no evidence for anomalous behavior. Perhaps moderate changes in orbits can have profound consequences on cometary mass loss.

3. Two of the brightening events occurred near the same point in the orbit on two separate orbits, near T_P+180 days in 2011 and 2018. Both events are long lived, and the comet remains at the higher activity level for at least several months. However, there is a lack of a similar event in 2003. A single active area may be responsible for all events, and appears to have been in relative quiescence in 2003.

We propose a scenario to account for these observations. The pre-2007 comet was near a steady state, balancing sublimation driven erosion with sub-surface devolatilization. The perihelion distance change perturbed this scenario, and warmed volatile-rich sub-surface layers that were previously insulated from the
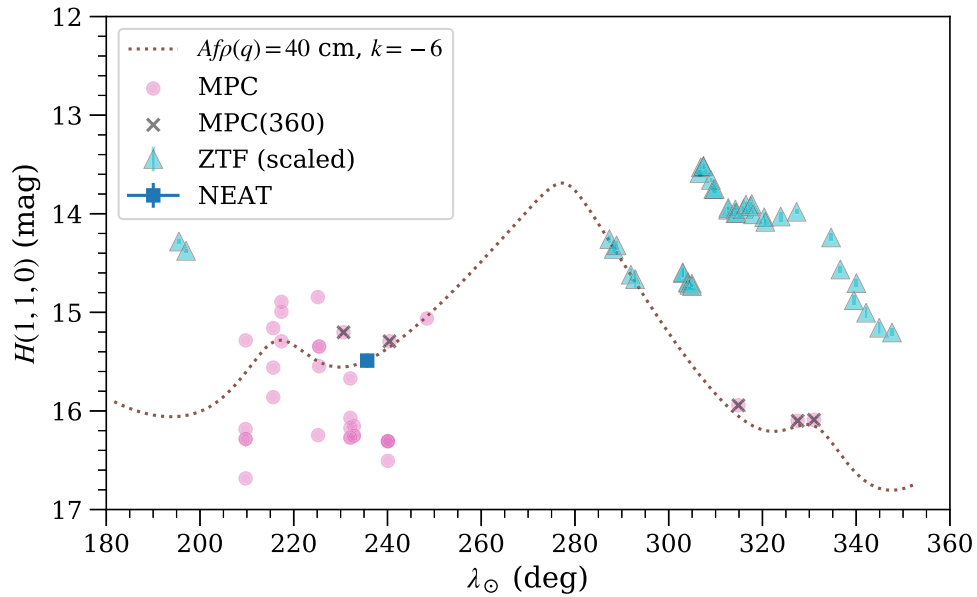
Figure 4. Absolute magnitude of comet 240P/NEAT from 2003 vs. ecliptic longitude of the comet–Sun vector. NEAT photometry within a $7''$ radius aperture, and select MPC photometry is shown. Photometry from Kuma Kogen Astronomical Observatory (MPC code 360), which observed both sides of perihelion, is highlighted. ZTF photometry from 2017 to 2018 is also shown, scaled to match the observation circumstances of 2003. The model lightcurve ($7''$ aperture, r_h^{-6} scale factor) was fit to the NEAT data point.

thermal wave. The new activity is isolated to one or two locations on the nucleus, indicating that the surface or immediate sub-surface is heterogeneous.

Terrain and activity heterogeneities are commonly observed by spacecraft missions to comets (A'Hearn et al. 2005, 2011; Veverka et al. 2013; Hässig et al. 2015; Thomas et al. 2015). The first observed transition (2010 orbit, $T_P + 182$ days) appears to have rejuvenated a local active area, perhaps shedding off an insulating layer. We speculate that the same surface is illuminated upon the approach to perihelion. Thus, the surface renewal may have occurred during the unobserved pre-perihelion approach in 2009. Tests of this idea would benefit from a pole orientation measurement. Thermophysical modeling of these events, and photometric observations during future perihelion passages will also help explore our proposed scenario.

Short-period comets, such as comet 240P, provide examples of cometary evolution from the cumulative effects of perihelion passages and orbital perturbations. After perturbations to smaller perihelion distances, comets may have a greater tendency toward enhanced activity levels (cometary rejuvenation), or the volatile reservoirs may quickly diminish (rapid surface mantling or devolatilization). Archival searches for comets under similar circumstances, and future comparisons to data taken with present-day surveys would benefit the study of comet behavior in general. We observed comet 240P at an interesting moment in its evolution. The pre-perihelion portion of the comet's 2025 orbit should be well observed with the Large Synoptic Survey Telescope, with science operations expected to begin in 2023.

ORCID iDs

Michael S. P. Kelley ⓘ https://orcid.org/0000-0002-6702-7676
Dennis Bodewits ⓘ https://orcid.org/0000-0002-2668-7248
Quanzhi Ye (叶泉志) ⓘ https://orcid.org/0000-0002-4838-7676
Tony L. Farnham ⓘ https://orcid.org/0000-0002-4767-9861
Eric C. Bellm ⓘ https://orcid.org/0000-0001-8018-5348
Dmitry A. Duev ⓘ https://orcid.org/0000-0001-5060-8733
George Helou ⓘ https://orcid.org/0000-0003-3367-3415
Thomas Kupfer ⓘ https://orcid.org/0000-0002-6540-1484
Russ R. Laher ⓘ https://orcid.org/0000-0003-2451-5482
Frank J. Masci ⓘ https://orcid.org/0000-0002-8532-9395
Thomas A. Prince ⓘ https://orcid.org/0000-0002-8850-3627
Ben Rusholme ⓘ https://orcid.org/0000-0001-7648-4142
David L. Shupe ⓘ https://orcid.org/0000-0003-4401-0430
Maayane T. Soumagnac ⓘ https://orcid.org/0000-0001-6753-1488

References

Agarwal, J., Della Corte, V., Feldman, P. D., et al. 2017, MNRAS, 469, s606
A'Hearn, M. F., Belton, M. J. S., Delamere, W. A., et al. 2005, Sci, 310, 258
A'Hearn, M. F., Belton, M. J. S., Delamere, W. A., et al. 2011, Sci, 332, 1396

A'Hearn, M. F., Schleicher, D. G., Millis, R. L., Feldman, P. D., & Thompson, D. T. 1984, AJ, 89, 579
Astropy Collaboration, Price-Whelan, A. M., Sipőcz, B. M., et al. 2018, AJ, 156, 123
Barbary, K. 2016, JOSS, 1, 58
Bauer, J. M., & Lawrence, K. J. 2013, Near Earth Asteroid Tracking V1.0, EAR-A-I1063-3-NEAT-V1.0, NASA Planetary Data System
Bellm, E. C., Kulkarni, S. R., Graham, M. J., et al. 2019, PASP, 131, 018002
Belton, M. J. S., & Melosh, J. 2009, Icar, 200, 280
Biver, N., Bockelee-Morvan, D., Colom, P., et al. 1997, Sci, 275, 1915
Bodewits, D., Farnham, T. L., A'Hearn, M. F., et al. 2014, ApJ, 786, 48
Cowan, J. J., & A'Hearn, M. F. 1979, M&P, 21, 155
Davidsson, B. J. R., Gutiérrez, P. J., Groussin, O., et al. 2013, Icar, 224, 154
El-Maarry, M. R., Thomas, N., Giacomini, L., et al. 2015, A&A, 583, A26
Farnham, T. L., Schleicher, D. G., Woodney, L. M., et al. 2001, Sci, 292, 1348
Feaga, L. M., A'Hearn, M. F., Farnham, T. L., et al. 2014, AJ, 147, 24
Fink, U., & Rubin, M. 2012, Icar, 221, 721
Graham, M. J., Kulkarni, S. R., Bellm, E. C., et al. 2019, PASP, 131, 078001
Groussin, O., sunshine, J. M., Feaga, L. M., et al. 2013, Icar, 222, 580
Gulkis, S., Allen, M., von Allmen, P., et al. 2015, Sci, 347, aaa0709
Gwyn, S. D. J., Hill, N., & Kavelaars, J. J. 2012, PASP, 124, 579
Hässig, M., Altwegg, K., Balsiger, H., et al. 2015, Sci, 347, aaa0276
Hayward, T. L., Hanner, M. S., & Sekanina, Z. 2000, ApJ, 538, 428
Hughes, D. W. 1990, QJRAS, 31, 69
Hughes, D. W. 1991, in IAU Coll. 116: Comets in the post-Halley Era 167, Astrophysics and Space Science Library, ed. R. L. Newburn, Jr., M. Neugebauer, & J. Rahe (Dordrecht: Kluwer), 825
Ishiguro, M., Kuroda, D., Hanayama, H., et al. 2016, AJ, 152, 169
Jewitt, D. C., & Meech, K. J. 1987, ApJ, 317, 992
Kelley, M. S. P., Bodewits, D., Ye, Q., et al. 2019, in ASP Conf. Ser. 523, Astronomical Data Analysis Software and Systems XXVIII, ed. P. Teuben (San Francisco: ASP)
Kelley, M. S. P., & Lister, T. 2019, Calviacat: Calibrate Star Photometry by Comparison to a Catalog, v1.0.2, Zenodo, doi:10.5281/zenodo.2635841
Knight, M. M., & Battams, K. 2014, ApJL, 782, L37
Kramer, T., Läuter, M., Rubin, M., & Altwegg, K. 2017, MNRAS, 469, S20
Laher, R. R., Surace, J., Grillmair, C. J., et al. 2014, PASP, 126, 674
Law, N. M., Kulkarni, S. R., Dekany, R. G., et al. 2009, PASP, 121, 1395
Lawrence, K. J., Bambery, R., Helin, E., et al. 2002, IAU Circ., 8029, 1
Li, J., & Jewitt, D. 2015, AJ, 149, 133
Masci, F. J., Laher, R. R., Rusholme, B., et al. 2019, PASP, 131, 018003
Meech, K. J., Yang, B., Kleyna, J., et al. 2013, ApJL, 776, L20
Ofek, E. O., Laher, R., Law, N., et al. 2012, PASP, 124, 62
Pajola, M., Höfner, S., Vincent, J. B., et al. 2017, NatAs, 1, 0092
Prialnik, D., & Bar-Nun, A. 1990, ApJ, 363, 274
Rau, A., Kulkarni, S. R., Law, N. M., et al. 2009, PASP, 121, 1334
Sato, H. 2017, CBET, 4427, 1
Schleicher, D. G. 2007, Icar, 190, 406
Schleicher, D. G., & Bair, A. N. 2011, AJ, 141, 177
Steckloff, J. K., & Samarasinha, N. H. 2018, Icar, 312, 172
Sunshine, J. M., Thomas, N., El-Maarry, M. R., & Farnham, T. L. 2016, JGRE, 121, 2194
Thomas, N., Sierks, H., Barbieri, C., et al. 2015, Sci, 347, aaa0440
Thomas, P., A'Hearn, M., Belton, M. J. S., et al. 2013, Icar, 222, 453
Tonry, J. L., Denneau, L., Heinze, A. N., et al. 2018, PASP, 130, 064505
Tonry, J. L., Stubbs, C. W., Lykke, K. R., et al. 2012, ApJ, 750, 99
Veverka, J., Klaasen, K., A'Hearn, M., et al. 2013, Icar, 222, 424
Williams, G. V. 2019, MPEC, 2019-J142, 1